INJECTION REQUIREMENTS FOR ELECTRON SWAP-OUT IN THE EIC-ESR*

Derong Xu†, William Bergan, Yi-Kai Kan, Yun Luo, Christoph Montag, Andrii Natochii,
Vahid Ranjbar, Manfred Wendt, Qiong Wu, Brookhaven National Laboratory, Upton, NY, USA

Abstract

The Electron–Ion Collider (EIC) will be the first collider to use electron swap-out injection to maintain high bunch polarization during operation. Meeting the EIC performance goals places stringent requirements on the Electron Storage Ring (ESR) injection process: the injected bunch must be introduced with minimal disturbance to the hadron beam, and electron losses must remain negligible to avoid detector background. This work summarizes the key ESR injection requirements, including orbit accuracy, injected emittance, and fast kicker requirements needed to meet the overall EIC performance requirements.

INTRODUCTION

The Electron-Ion Collider (EIC) is a next-generation nuclear physics facility designed to explore the structure of nucleons and nuclei with unprecedented precision [1]. It will deliver collisions of highly polarized electron and ion beams over a wide range of center-of-mass energies, with key performance parameters including electron average polarization of about 70 % and luminosities of 10^{33-34} $\mathrm{cm^{-2}s^{-1}}$ [2].

To meet these performance goals, the Electron Storage Ring (ESR) must be provided with electron bunches of high charge and high polarization over a broad energy range. This is achieved through a dedicated electron injector chain, as shown in Fig. 1, consisting of a polarized electron source and linac, a Beam Accumulator Ring (BAR), and a Rapid Cycling Synchrotron (RCS). The BAR accumulates bunch charge up to 28 nC, and the RCS accelerates the beam while preserving polarization.

Once stored in the ESR, the electron beam polarization decays over time. Maintaining a high average polarization therefore requires frequent replacement of electron bunches, and the EIC adopts a single-bunch swap-out injection scheme for bunch-by-bunch polarization management. To sustain high luminosity, injection into the ESR must take place during ongoing collisions with the hadron beam. The hadron beam has no effective cooling, so any emittance growth accumulates. In a charge accumulation scheme, sufficient separation between the stored and injected electron bunches is required, which introduces transient perturbations to the hadron beam and leads to emittance growth [3]. In contrast, in the ideal limit where each stored electron bunch is directly replaced by a fresh one without mismatch or errors, the swap-out process provides an intrinsically transparent environment for the hadron beam [4].

* Work supported by Brookhaven Science Associates, LLC under Contract No. DE-SC0012704 with the U.S. Department of Energy
† dxu@bnl.gov

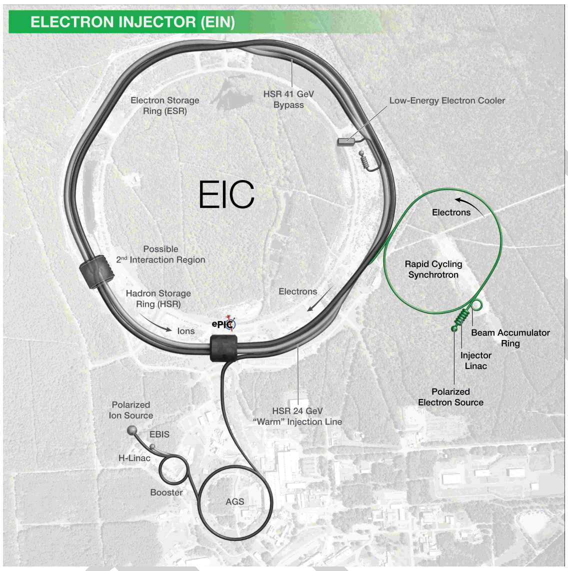

Figure 1: Overview of the EIC facility. The electron injector chain (colored) includes the polarized electron source and linac, BAR, and RCS, delivering electron bunches to the ESR (black).

However, injection errors are unavoidable in practice, and the acceptable hadron beam emittance growth defines the tolerances on injection imperfections. Swap-out injection has been established in modern storage rings such as the APS-U [5], demonstrating the feasibility of high-charge swap-out operation. The focus of this work is to quantify these tolerances for the EIC ESR under its unique operating conditions involving simultaneous injection and collision.

ESR DESIGN CONSTRAINTS

The ESR is designed to operate at multiple energies [6], specifically 5 GeV and 10 GeV, with upgrade capability to 18 GeV, to satisfy the center-of-mass energy requirements.

The physics program requires simultaneous storage of both spin states in the ESR, with a random spin pattern. Due to the Sokolov–Ternov effect, the spin component aligned with the magnetic field in the arcs exhibits a faster polarization decay. Table 1 lists the corresponding constraints for different energies and spin states.

The most stringent requirement arises at 18 GeV, where the shortest replacement interval in Table 1 sets the timescale for bunch replacement and determines the required injection frequency. In addition, to avoid significant loss of integrated luminosity, the initial fill should be completed within 20 min for all electron bunches. Considering both constraints, an injection frequency of 1 Hz is chosen.

Table 1: ESR operating parameters to satisfy the EIC key performance requirements. The maximum replacement interval T_{rep} is defined as the longest allowed time between bunch replacements to maintain an average polarization above 70 %.

Parameter	unit	5 GeV	10 GeV	18 GeV
Bunches	–	1160	1160	290
Charge	nC	28	28	11
T_{rep} (up)	min	150	96	4
T_{rep} (down)	min	232	359	11.5
T_{rep}(avg)	min	182	151	6

The peak luminosity configuration corresponds to collisions between 275 GeV protons and 10 GeV electrons, which defines the reference scenario for the following tolerance analysis. Under a 1 Hz injection frequency, the replacement cycle over all bunches is about 20 min, during which a proton bunch collides with the same electron bunch before it is replaced.

The allowable proton vertical emittance growth is limited to 70 %/h to preserve high integrated luminosity. Considering that multiple sources of noise contribute to emittance growth (e.g., [7, 8]), the total growth budget must be shared among these contributions, including those from electron injection. For an injection frequency of 1 Hz, this corresponds to a per-injection growth budget at the percent level. A conservative threshold of 1 % relative emittance growth per injection is therefore adopted to determine the tolerance for each type of injection error in the following sections.

PHASE-SPACE MISMATCH

The injected electron bunch may deviate from the equilibrium distribution of the ESR in six-dimensional phase space. Such deviations include offsets in all six coordinates, as well as mismatch in transverse and longitudinal emittances.

In the ideal case, where the injected beam is perfectly matched in orbit, momentum, and emittance, the proton emittance growth per injection is below 0.1 % and can be neglected.

In the presence of phase-space mismatch, the injected electron distribution evolves toward equilibrium. The mismatch initially induces orbit and envelope oscillations. Due to the strong and nonlinear beam-beam interaction, the large tune spread rapidly destroys coherent motion within $\mathcal{O}(10^2)$ turns. At longer timescales, synchrotron radiation damping drives the distribution toward a new equilibrium.

This transient evolution introduces two main effects: proton emittance growth and electron beam loss.

The EIC employs a flat hadron beam to maximize luminosity, with a vertical emittance an order of magnitude smaller than the horizontal one [9]. This small vertical emittance is sensitive to external perturbations. Phase-space mismatch of the electron beam modifies the beam-beam force acting on the proton beam, leading to emittance growth.

A systematic scan over six-dimensional phase-space deviations is performed using self-consistent strong-strong simulations. The resulting tolerances, defined by requiring the relative proton emittance growth to remain below 1 % per injection, are summarized in Table 2, where all errors are normalized to the ESR design values.

Table 2: Allowable phase-space mismatch errors corresponding to a 1 % proton emittance growth per replacement. The errors are normalized by ESR design value. The symbols “>” and “<” indicate that the actual bounds lie beyond the parameter range explored in the simulation.

Parameter	Lower Bound	Upper Bound
Δx	$-0.6\sigma_x$	$0.6\sigma_x$
Δp_x	$-0.7\sigma_x'$	$0.7\sigma_x'$
$\epsilon_{x,\mathrm{inj}}$	$0.8\epsilon_x$	$> 2\epsilon_x$
Δy	$-1.5\sigma_y$	$1.5\sigma_y$
Δp_y	$-0.9\sigma_y'$	$0.9\sigma_y'$
$\epsilon_{y,\mathrm{inj}}$	$0.6\epsilon_y$	$> 5\epsilon_y$
Δz	$-1.3\sigma_z$	$1.3\sigma_z$
Δp_z	$-1.3\sigma_\delta$	$1.3\sigma_\delta$
$\epsilon_{z,\mathrm{inj}}$	$< \epsilon_z/3$	$> 3\epsilon_z$

Electron losses reduce luminosity and may contribute to detector background. At 10 GeV, a safe loss rate is approximately 5×10^6 electrons per second within the detector region, based on beam-gas and Touschek scattering studies [10]. This corresponds to a fractional loss per injection of $\sim 10^{-6}$.

To estimate the loss induced by injection errors, we conservatively assume that all lost particles are confined within the interaction region (IR). The loss probability is then evaluated by integrating the injected phase-space distribution within the ESR acceptance.

The acceptance is approximated using the ESR dynamic aperture target [11], together with the longitudinal RF bucket constraint. Figure 2 shows an example of the dependence of electron loss on the horizontal emittance, with other mismatch parameters set to zero.

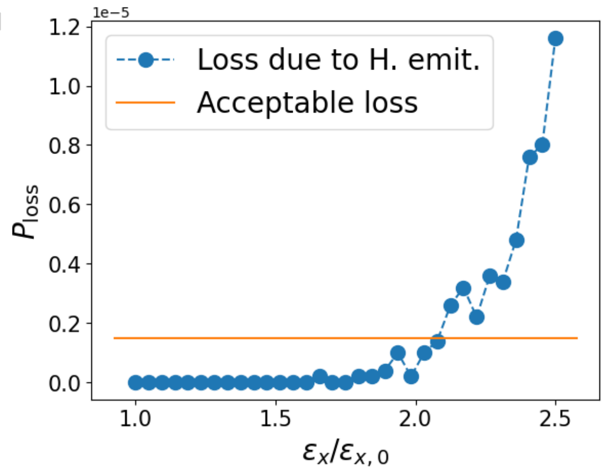

Figure 2: Electron loss probability as a function of horizontal emittance. The orange line indicates the acceptable range corresponding to $P_{loss} < 1.5 \times 10^{-6}$.

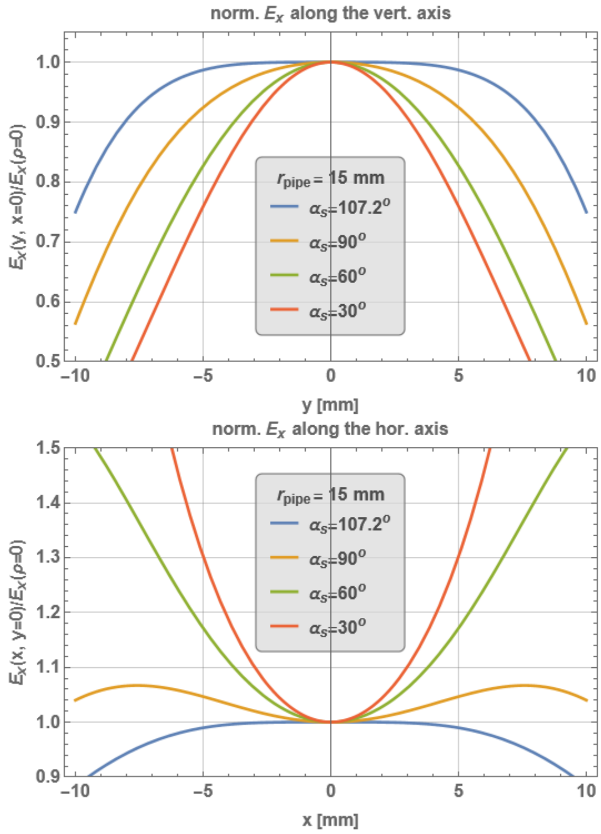

Figure 3: Transverse E_x field inhomogeneity of the ESR injection kicker within a ± 10 mm range for different electrode coverage angles.

FAST STRIPLINE KICKER ERRORS

The fast kicker is an essential component for implementing single-bunch swap-out injection in the ESR. It provides the transverse deflection required to place the injected electron bunch onto the design orbit, while simultaneously extracting the stored bunch. Fast kicker errors introduce additional perturbations to the injected bunch distribution, which in turn affect the proton beam through the beam-beam interaction.

One source of error arises from the transverse non-uniformity of the kicker field. Particles at larger transverse amplitudes experience deviations from the nominal kick. The magnitude of this effect depends on the stripline electrode coverage angle. Larger coverage improves field uniformity and reduces kick errors, while smaller coverage leads to stronger non-uniformity. Figure 3 shows the transverse field distribution for different electrode coverage angles [12]. The choice of electrode coverage therefore represents a trade-off between kick quality and beam-induced heating, as narrower electrodes are preferred from the perspective of wakefields and thermal load.

To evaluate the impact of non-uniform kick, four kick models in Fig. 3 are incorporated into a self-consistent strong-strong simulation. The results show that the electron beam undergoes emittance blow-up, which becomes more pronounced for larger β_x at the injection point. A smaller β_x reduces the transverse beam size, thereby limiting the fraction of particles that sample large field errors. The proton beam exhibits a small emittance increase during each bunch replacement, with the magnitude remaining within the 1 % acceptable level.

To limit the electron emittance blow-up, constraints on the horizontal beta function at the injection point are obtained. For a 107° electrode, no limitation is observed up to β_x = 90 m. For a 90° electrode, the requirement becomes $\beta_x \leq$ 30 m, while for narrower electrodes (60° or 30°), β_x must be reduced to $\leq$ 10 m.

Another source of error arises from the fall time of the fast kicker. The residual field produces a ~3 % kick on the following bunch. For the given injection optics, this residual kick corresponds to a horizontal offset exceeding 1σ, which leads to a proton vertical emittance growth greater than 2 % per injection. This effect therefore must be mitigated through the kicker design.

COMBINED INJECTION ERRORS

Non-uniform kicker fields introduce additional transverse perturbations to the injected bunch, effectively reducing the tolerance of the phase-space offset and angle errors. To obtain a realistic estimate of the tolerance, these effects are incorporated into the injection model together with the injection optics.

The transverse emittances of the injected electron beam are fixed to twice the ESR design values, based on estimates from the RCS extraction, while the longitudinal parameters follow the RCS design values. A 2π phase advance is assumed between the injection point and the beam-beam interaction point. The allowable ranges of phase-space errors are determined by requiring both 1 % proton emittance growth per injection and an electron loss probability below 1.5×10^{-6}. The results are summarized in Table 3.

Table 3: Allowable phase-space mismatch errors determined by a 1 % proton emittance growth per injection and 1.5×10^{-6} electron loss. The errors are normalized by ESR design values. Realistic injection optics and RCS extraction emittance are assumed.

Parameter	Lower Bound	Upper Bound
Δx	$-0.4\sigma_x$	$0.4\sigma_x$
Δp_x	$-0.7\sigma'_x$	$0.7\sigma'_x$
Δy	$-1.5\sigma_y$	$1.5\sigma_y$
Δp_y	$-0.9\sigma'_y$	$0.9\sigma'_y$
Δz	$-1.3\sigma_z$	$1.3\sigma_z$
Δp_z	$-1.3\sigma_\delta$	$1.3\sigma_\delta$

SUMMARY

Injection errors in the ESR, including phase-space mismatch and fast kicker imperfections, can induce proton emittance growth and electron loss. This study estimates injection error tolerances for EIC ESR swap-out injection, providing guidance for the ESR injection design.

REFERENCES

[1] A. Accardi *et al.*, "Electron Ion Collider: The Next QCD Frontier: Understanding the glue that binds us all", *Eur. Phys. J. A*, vol. 52, no. 9, p. 268, 2016. doi:10.1140/epja/i2016-16268-9

[2] F. Willeke *et al.*, "Electron Ion Collider Conceptual Design Report 2021", Feb. 2021. doi:10.2172/1765663

[3] D. Xu *et al.*, "Advancing electron injection dynamics and mitigation approaches in the electron-ion collider's swap-out injection scheme", in *Proc. IPAC'24*, Nashville, TN, USA, May 2024, pp. 230–233. doi:10.18429/JACoW-IPAC2024-MOPC72

[4] J. Qiang *et al.*, "Transient Beam-Beam Effect During Electron Bunch Replacement in the EIC", in *Proc. IPAC'21*, Campinas, SP, Brazil, May 2021, pp. 3228–3231. doi:10.18429/JACoW-IPAC2021-WEPAB252

[5] V. Sajaev *et al.*, "Aps upgrade: commissioning the world's first light source based on swap-out injection", in *Proc. NA-PAC'25*, Sacramento, CA, USA, Aug. 2025, pp. 1–6. doi:10.18429/JACoW-NAPAC2025-MOXP02

[6] D. Marx *et al.*, "Designing the EIC Electron Storage Ring Lattice for a Wide Energy Range", in *Proc. IPAC'22*, Bangkok, Thailand, Jun. 2022, pp. 1946–1949. doi:10.18429/JACoW-IPAC2022-WEPOPT042

[7] D. Xu *et al.*, "Effect of electron orbit ripple on proton emittance growth in eic", in *Proc. IPAC'23*, Venice, Italy, May 2021, pp. 108–111. doi:10.18429/JACoW-IPAC2023-MOPA039

[8] Y. Luo *et al.*, "Weak-strong beam-beam simulation with crab cavity noises for the hadron storage ring of the electron-ion collider", in *Proc. IPAC'24*, Nashville, TN, USA, May 2024, pp. 250–253. doi:10.18429/JACoW-IPAC2024-MOPC78

[9] Y. Luo, D. Xu, M. Blaskiewicz, and C. Montag, "Experimental demonstration of a large transverse emittance ratio 11 : 1 in the relativistic heavy ion collider for the electron-ion collider", *Phys. Rev. Lett.*, vol. 132, no. 20, p. 205001, May 2024. doi:10.1103/PhysRevLett.132.205001

[10] A. Natochii and E. Aschenauer, "Private communication", Brookhaven National Laboratory, Upton, NY, USA, 2025,

[11] Y. Cai *et al.*, "Optimization of chromatic optics in the electron storage ring of the electron-ion collider", *Phys. Rev. Accel. Beams*, vol. 25, no. 7, p. 071001, Jul. 2022. doi:10.1103/PhysRevAccelBeams.25.071001

[12] M. Wendt, "Private communication", Brookhaven National Laboratory, Upton, NY, USA, 2024,